Entropy propagation analysis in stochastic structural dynamics: application to a beam with uncertain cross sectional area

Anas Batou, T. G. Ritto, Rubens Sampaio

Entropy propagation analysis in stochastic structural dynamics: Application to a beam with uncertain cross sectional area

A. Batou · T.G. Ritto · Rubens Sampaio

Abstract This paper investigates the impact of different probabilistic models of uncertain parameters on the response of a dynamical structure. The probabilistic models of the uncertain parameters are constructed using the Maximum Entropy principle, where different information is considered, such as bounds, mean value, etc. Nested probabilistic models are constructed with increasing information; as the information given increases, the level of entropy of the input model decreases. The response of the linear dynamical model is given in the frequency domain, and the propagation of the input uncertainty throughout the computational model is analyzed in terms of Shannon's entropy. Low and high frequencies are analyzed because uncertainties propagate differently depending on the frequency band. A beam discretized by means of the finite element method with random cross sectional area (random field) is the application analyzed.

A. Batou
Laboratoire de Modélisation et Simulation Multi Echelle, MSME UMR 8208, Université Paris-Est, 5 bd Descartes, 77454 Marne-la-Vallée, France.
E-mail: anas.batou@univ-paris-est.fr

T. G. Ritto
Federal University of Rio de Janeiro, Department of Mechanical Engineering, Centro de Tecnologia, Ilha do Fundão, 21945-970, Rio de Janeiro, Brazil.
E-mail: tritto@mecanica.ufrj.br

Rubens Sampaio
PUC-Rio, Department of Mechanical Engineering, Rua Marquês de São Vicente, 225, 22453-900, Rio de Janeiro, Brazil.
E-mail: rsampaio@puc-rio.br

1 Introduction

This research concerns the prediction of the dynamical response of a structure in the presence of parameter uncertainties. These uncertainties are related to the variability appearing during the manufacturing process or during the cycle life (uncontrolled damages) of the structure. These uncertainties propagates into the response of the structure yielding more or less uncertainties in the quantities of interest. If these output uncertainties are non-negligible, then they have to be taken into account in order to predict the dynamical response and support decision makers.

In the context of the probabilistic methods for uncertainty quantification, the uncertain parameters are replaced by random variables. Then, the first step consists in constructing a probabilistic model for these parameters, i.e., construct the probability density functions (pdf) for the random variables modelling the uncertain parameters. The Shannon entropy [15] measures the relative uncertainty associated to a pdf. The Maximum Entropy (MaxEnt) principle [15,4,5] in the context of Information Theory is a powerful method which allows the pdf of a random variable to be constructed from a set of available information. This method consists in choosing the pdf which maximizes the entropy (and thus the uncertainty) under the constraints defined by the available information. Therefore, the entropy (uncertainty) level in the input parameters depends on the amount of information available for the uncertain parameters. It is then interesting to analyse how this level of entropy propagates into the quantities of interest.

Usually, the propagation of uncertainties is analysed through the observation of the input/output variance. Indeed, in general, the variance increases if the uncertainty related to a probability distribution increases. Nevertheless, in some specific cases (for instance, a bi-modal distribution for which the distance between the two peaks is large), a probability distribution with low uncertainty can have a large variance. Then for these specific cases, the variance is not a reliable measure of uncertainty. For this reason entropy-based sensitivity indexes have been introduced in [10] as an alternative to the classical Sobol indexes [16] which are variance-based. Entropy measures were also recently used for identification of structural dynamics and damage detection. In [12] the transfer entropy measure was used for damage detection in a simple discrete dynamical system and in [1] a relative entropy measure was used to perform an inverse problem in a beam structure.

In the present paper, we provide a general methodology to analyze the input-entropy propagation into the dynamical response of a structure. Such an analysis is important in order to quantify the effects of the probabilistic modelling of the input parameters on the uncertainty related to the output quantities of interest. Then such an analysis can provide important information related to (1) the sensitivity of the outputs with respect to the variability of the inputs (this information can be obtained using a classical variance-based sensitivity analysis) and (2) the robustness of the output variability with respect to the choice of the input probability model. If this robustness is good enough

then a coarse probabilistic modelling of the input parameters is sufficient in order to predict the random dynamical response with a good robustness. This latter point is important in order to determine the quantity of information that is needed for the construction of the input probability model. For instance, if a uniform distribution and a beta distribution for the inputs have the same effect on the output then the uniform distribution will be preferred since it only require the bounds of the inputs (given by the manufacturing tolerances). On the contrary, if the effect of the input probability model on the output variability is not negligible, then it is important to analyze if the decrease of the input entropy induces a decrease or an increase of the output entropy. In the latter case a fine input probability model (constructed using a large amount of information) is required in order to avoid an underestimation of the output uncertainty (measured by the output entropy).

The objectives and contributions of the present papers are: (1) provide a general methodology to analyze the propagation of uncertainty throughout a linear dynamical structure in terms of input/output entropy, (2) analyze how increasing entropy in the probabilistic model of the parameters affects the entropy of the response; for this purpose, nested input probabilistic models are constructed using the Maximum Entropy principle, and (3) analyze the uncertainty propagation in low and high frequencies to highlight the stochastic homogenisation that can occur for the random response in the low frequency band.

This paper is organized as follows. In Section 2, the reduced-order nominal computational model is constructed. Then, Section 3 is devoted to (1) the construction of the stochastic computational which is derived from the reduced nominal computational model and (2) the estimation of the output entropy. Finally, in Section 4, an application related to the random response of an Euler beam with random cross sectional area (random field) is presented.

2 Reduced nominal computational model

In this section the reduced nominal computational model is constructed using the Finite Element method and the model reduction is performed using a classical modal analysis.

2.1 Nominal computational model

We are interested in the dynamical response of a three-dimensional damped structure having a linear behavior. This structure is made up of a linear dissipative elastic medium occupying an open bounded domain Ω, with boundary $\partial\Omega = \Gamma_0 \cup \Gamma$. Let $\mathbf{x}$ be the coordinates of a point in Ω. The external unit normal to $\partial\Omega$ is denoted by $\mathbf{n}$. Let $\mathbf{u}(\mathbf{x}, \omega)$ be the displacement field defined in the frequency domain with values in $\mathbf{C}^3$. We assume that $\mathbf{u} = 0$ on part Γ_0 and, consequently, there is no rigid body displacements. Let the vector $\mathbf{f}^{\,\mathrm{surf}}(\mathbf{x}, \omega)$

denote the surface force field applied on the boundary Γ and let the vector $\mathbf{f}^{\text{vol}}(\mathbf{x}, \omega)$ denote the volume force field applied in Ω. We are interested in the linear response around a static equilibrium considered as the reference configuration defined by Ω. The boundary value problem in the frequency domain is written, for all ω, as

$$
\begin{aligned}
-\omega^2 \rho \, \mathbf{u} - \operatorname{div} \boldsymbol{\sigma} &= \mathbf{f}^{\text{vol}} \text{ in } \Omega \,, \\
\mathbf{u} &= \mathbf{0} \qquad \text{on } \Gamma_0 \,, \\
\boldsymbol{\sigma} \, \mathbf{n} &= \mathbf{f}^{\text{surf}} \qquad \text{on } \Gamma \,,
\end{aligned}
\tag{1}
$$

where $\rho(\mathbf{x})$ is the mass density and $\boldsymbol{\sigma}(\mathbf{x}, \omega)$ is the second-order stress tensor, in which $\{\operatorname{div} \boldsymbol{\sigma}(\mathbf{x}, \omega)\}_j = \sum_{k=1}^{3} \partial \sigma_{jk}(\mathbf{x}, \omega)/\partial x_k$. The stress tensor $\boldsymbol{\sigma}(\mathbf{x}, \omega)$ will be related to the strain tensor $\boldsymbol{\varepsilon}(\mathbf{x}, \omega)$ by a constitutive equation which is written for a non-homogeneous anisotropic dissipative elastic medium as $\sigma_{h\ell}(\mathbf{x}, \omega) = a_{h\ell jk}(\mathbf{x}) \, \varepsilon_{jk}(\mathbf{x}, \omega) + i\omega \, b_{h\ell jk}(\mathbf{x}) \, \varepsilon_{jk}(\mathbf{x}, \omega)$ in which $a_{h\ell jk}(\mathbf{x})$ and $b_{h\ell jk}(\mathbf{x})$ are the fourth-order real tensors related to the elastic and dissipative parts and which must satisfy symmetry and positiveness properties.

In this paper, in order to improve the readability, we are analyzing only one parameter field of interest which is denoted by $\mathbf{x} \mapsto \text{h}(\mathbf{x})$. The generalization for several parameter fields is straightforward. The parameters can be material parameters such as the mass density or the Lame parameters, or other model parameters such as the section for a beam model, the thickness for a plate model, etc.

The computational model is constructed using the finite element (FE) method applied to the weak formulation of the dynamical problem defined by Eq. (1). Let $\mathbf{x}^1, \dots, \mathbf{x}^N$ be the set of the N positions where the field $\text{h}(\mathbf{x})$ is discretized. These positions can correspond to the integration points of the FE model. If the mesh is sufficiently fine the field $\text{h}(\mathbf{x})$ can be assumed as constant in each element and the discretizations points are the barycenters of the elements. Let $\mathbf{h} = (\text{h}(\mathbf{x}^1), \dots, \text{h}(\mathbf{x}^N)) \in \text{R}^N$ be the vector of the discretized system parameters, that latter will be replaced by a random vector (see Section 3).

We are interested in the frequency response of the structure on the frequency band of analysis $B = [0, \omega_{max}]$. Let m be the total number of degrees-of-freedom in the FE model. For all $\omega \in B$, the vector $\mathbf{y}(\omega) \in \text{R}^m$ of the m degrees-of-freedom is the solution of the following matrix equation

$$
(-\omega^2 [\text{M}(\mathbf{h})] + i\omega [\text{D}(\mathbf{h})] + [\text{K}(\mathbf{h})]) \, \mathbf{y}(\omega) = \widetilde{\mathbf{f}}(\omega) \,,
\tag{2}
$$

in which $[\text{M}(\mathbf{h})]$, $[\text{D}(\mathbf{h})]$ and $[\text{K}(\mathbf{h})]$ are the $(m \times m)$ mass, damping and stiffness matrices and where $\widetilde{\mathbf{f}}(\omega)$ is the vector of the external forces.

2.2 Reduced-order nominal computational model

The reduced nominal computation model is constructed using the modal analysis reduction method. Let $\mathcal{C}_h$ be the admissible set for the vector $\mathbf{h}$. Then for

all $\mathbf{h}$ in $\mathcal{C}_h$, the n first eigenvalues $0 < \lambda_1(\mathbf{h}) \leq \lambda_2(\mathbf{h}) \leq \ldots \leq \lambda_n(\mathbf{h})$ associated with the elastic modes $\{\phi_1(\mathbf{h}), \phi_2(\mathbf{h}), \ldots, \phi_n(\mathbf{h})\}$ are solutions of the following generalized eigenvalue problem

$$[\mathrm{K}(\mathbf{h})]\,\phi(\mathbf{h}) = \lambda(\mathbf{h})[\mathrm{M}(\mathbf{h})]\,\phi(\mathbf{h})\,. \tag{3}$$

The reduced-order nominal computation model is obtained by projecting the nominal computation model on the subspace spanned by the n first elastic modes calculated using Eq. (3). Let $[\Phi(\mathbf{h})]$ be the $m \times n$ matrix whose columns are the n first elastic modes. We then introduce the approximation

$$\mathbf{y}(\omega) = [\Phi(\mathbf{h})]\,\mathbf{q}(\omega)\,, \tag{4}$$

in which the vector $\mathbf{q}(\omega)$ is the vector of the n generalized coordinates and is the solution of the following reduced matrix equation

$$(-\omega^2[\widetilde{M}(\mathbf{h})] + i\omega[\widetilde{D}(\mathbf{h})] + [\widetilde{K}(\mathbf{h})])\,\mathbf{q}(\omega) = \mathbf{f}(\omega; \mathbf{h})\,, \tag{5}$$

in which $[\widetilde{M}(\mathbf{h})] = [\Phi(\mathbf{h})]^T\,[\mathrm{M}(\mathbf{h})]\,[\Phi(\mathbf{h})]$, $[\widetilde{D}(\mathbf{h})] = [\Phi(\mathbf{h})]^T\,[\mathrm{D}(\mathbf{h})]\,[\Phi(\mathbf{h})]$ and $[\widetilde{K}(\mathbf{h})] = [\Phi(\mathbf{h})]^T\,[\mathrm{K}(\mathbf{h})]\,[\Phi(\mathbf{h})]$ are the $n \times n$ mass, damping and stiffness generalized matrices, and where $\mathbf{f}(\omega; \mathbf{h}) = [\Phi(\mathbf{h})]^T\,\widetilde{\mathbf{f}}(\omega) \in \mathrm{R}^n$ is the vector of the generalized forces. The random response is calculated at n_{freq} frequencies belonging to frequency band B. We then introduce the observation vector $\mathbf{z} = OBS(\mathbf{y}(\omega_1), \ldots, \mathbf{y}(\omega_{n_{\mathrm{freq}}}))$ in $\mathrm{R}^{n_{\mathrm{obs}}}$, where n_{obs} is the number of outputs observed.

3 Stochastic computational model

In this section, the stochastic computational model is derived from the reduced-order nominal computational model introduced in the previous section. The random variables, the random vectors and the random fields are denoted using uppercase letters. The uncertain parameter field of the dynamical system is modeled by a random field, which means that the field $\{\mathrm{h}(\mathbf{x}), \mathbf{x} \in \Omega\}$ is modeled by the random field $\{\mathrm{H}(\mathbf{x}), \mathbf{x} \in \Omega\}$. Furthermore, it is assumed that the random field $\{\mathrm{H}(\mathbf{x}), \mathbf{x} \in \Omega\}$ is homogeneous. Therefore, in the context of the FE discretization introduced in the previous section, the vector $\mathbf{h}$ which corresponds to the spatial discretization of $\mathrm{h}(\mathbf{x})$, is modeled by a random vector $\mathbf{H}$. The probabilistic model of this random vector is constructed using the MaxEnt principle. Finally, the stochastic reduced-order computational model is presented.

3.1 Probabilistic model of uncertainties

In this section, the probability distribution of the random vector $\mathbf{H}$ is constructed using the MaxEnt principle. Two general cases are considered. For the first case, the available information is introduced independently for each

component of the random vector $\mathbf{H}$ yielding independent components for the random vector $\mathbf{H}$. For the second case, additional constraints related to the correlation between components are introduced yielding a dependence between these components.

3.1.1 Independent information case

For this particular case, the random variable $\mathbf{H}$ is denoted $\mathbf{H}^{\mathrm{nc}}$. The available information is introduced independently for each component of the random vector $\mathbf{H}^{\mathrm{nc}}$. Since it is assumed that the random field $\{\mathrm{H}(\mathbf{x}), \mathbf{x} \in \Omega\}$ is homogeneous, the available information is the same for all the components of the random vector $\mathbf{H}^{\mathrm{nc}}$. The support of the pdf of each component H_i^{nc} is denoted by $\mathcal{K}$ such that $\mathcal{K} \subset \mathrm{R}$. The available information for the components H_i^{nc} are related to physical properties or available statistics on this components. For each component, H_i^{nc}, $i = 1, \ldots, N$, the available information is written as the following μ constraints

$$E\{\mathbf{g}(H_i^{\mathrm{nc}})\} = \mathbf{f}\,, \tag{6}$$

in which $h \mapsto \mathbf{g}(h)$ is a given function from R into R^μ, $E\{.\}$ is the mathematical expectation, and $\mathbf{f}$ is a given vector in R^μ. Equation (6) can be rewritten as

$$\int_{\mathrm{R}} \boldsymbol{g}(h_i) p_{h_i^{\mathrm{nc}}}(h_i) \mathrm{d}h_i = \mathbf{f}\,. \tag{7}$$

An additional constraint related to the normalization of the joint pdf $p_{\mathbf{H}^{\mathrm{nc}}}(\mathbf{h})$ is introduced such that

$$\int_{\mathrm{R}^N} p_{\mathbf{H}^{\mathrm{nc}}}(\mathbf{h}) \mathrm{d}\boldsymbol{h} = 1\,. \tag{8}$$

It should be noted that the available information in Eq. (6) is restricted to expectations of given functions. Therefore, the MaxEnt principle does not allow taking into account almost sure properties of given realizations of the random variables. The Shannon entropy of the joint pdf $\mathbf{h} \mapsto p_{\mathbf{H}^{\mathrm{nc}}}(\mathbf{h})$ is defined by

$$S(p_{\mathbf{H}^{\mathrm{nc}}}) = -\int_{\mathrm{R}^N} p_{\mathbf{H}^{\mathrm{nc}}}(\mathbf{h})\,\log(p_{\mathbf{H}^{\mathrm{nc}}}(\mathbf{h}))\mathrm{d}\mathbf{h}\,, \tag{9}$$

where log is the natural logarithm. This functional measures the uncertainty associated with $p_{\mathbf{H}^{\mathrm{nc}}}(\mathbf{h})$. Let $\mathcal{C}$ be the set of all the pdf defined on R^N with values in R^+, verifying the constraints defined by Eqs. (7) and (8). Then the MaxEnt principle consists in constructing the probability density function $\boldsymbol{h} \mapsto p_{\mathbf{H}^{\mathrm{nc}}}(\mathbf{h})$ as the unique pdf in $\mathcal{C}$ which maximizes the entropy $S(p_{\mathbf{H}^{\mathrm{nc}}})$. By introducing a Lagrange multiplier λ_0 in R^+ associated with Eq. (8) and N Lagrange multipliers $\boldsymbol{\lambda}_i$ associated with Eq. (7) and belonging to an admissible open subset $\mathcal{L}_\mu$ of R^μ, it can be shown [4,5] that the MaxEnt solution, if it exists, is defined by

$$p_{\mathbf{H}^{\mathrm{nc}}}(\mathbf{h}) = \prod_{i=1}^{N} \{\mathbb{1}_{\mathcal{K}}(h_i)\} \, c_0^{\mathrm{sol}} \, \exp(-\sum_{i=1}^{N} \langle \boldsymbol{\lambda}_i^{\mathrm{sol}}, \mathbf{g}(h_i) \rangle) \,, \tag{10}$$

in which the indicator function $h_i \mapsto \mathbb{1}_{\mathcal{K}}(h_i)$ is such that it is equal to 1 if $h_i \in \mathcal{K}$ and is zero otherwise. In Eq. (10), $c_0^{\mathrm{sol}} = \exp(-\lambda_0^{\mathrm{sol}})$, $\langle \boldsymbol{x}, \boldsymbol{y} \rangle = x_1 y_1 + \ldots + x_\mu y_\mu$ and λ_0^{sol} and $\boldsymbol{\lambda}_i^{\mathrm{sol}}$ are respectively the values of λ_0 and $\boldsymbol{\lambda}_i$ for which Eqs. (7) and (8) are satisfied. Equation (10) shows that the components h_i of the the random vector $\mathbf{H}$ are independent random variables for which the pdfs are given for i in $\{1, \ldots, N\}$ by

$$p_{H_i^{\mathrm{nc}}}(h_i) = \mathbb{1}_{\mathcal{K}}(h_i) \, c_i^{\mathrm{sol}} \, \exp(-\langle \boldsymbol{\lambda}_i^{\mathrm{sol}}, \mathbf{g}(h_i) \rangle) \,. \tag{11}$$

This result is obvious and could be stated at the beginning by applying the MaxEnt principle on each component independently. Using the normalization condition, the parameter c_i^{sol} can be eliminated and Eq. (11) can be rewritten as

$$p_{H_i^{\mathrm{nc}}}(h_i) = \mathbb{1}_{\mathcal{K}}(h_i) \, c_i(\boldsymbol{\lambda}_i^{\mathrm{sol}}) \, \exp(-\langle \boldsymbol{\lambda}_i^{\mathrm{sol}}, \mathbf{g}(h_i) \rangle) \,, \tag{12}$$

in which $c_i(\boldsymbol{\lambda_i})$ is defined by

$$c_i(\boldsymbol{\lambda_i}) = \left\{ \int_{\mathcal{K}} \exp(-\langle \boldsymbol{\lambda}_i, \boldsymbol{g}(h_i) \rangle) \, \mathrm{d}h_i \right\}^{-1} \,. \tag{13}$$

The N Lagrange multipliers $\boldsymbol{\lambda}_i$ are then calculated using Eqs. (7), (12) and (13). The integrals can be calculated explicitly for some particular cases of available information. Since, the dimension of these integrals is one, they can be calculated using any numerical integration method.

If we consider that the support $\mathcal{K}$ is compact then, if no available information is introduced, the MaxEnt distribution is the uniform distribution. Hence, if an available information is added, a constraint is added and the research manifold for the maximum of the entropy is reduced yielding a smaller maximum. More specifically, if we introduce the two random variables H^1 and H^2, with the same support, for which the available information are respectively defined by

$$E\{\boldsymbol{g}^1(H^1)\} = \boldsymbol{f}^1 \,, \tag{14}$$

$$E\{\boldsymbol{g}^1(H^2)\} = \boldsymbol{f}^1 \,, \; E\{\boldsymbol{g}^2(H^2)\} = \boldsymbol{f}^2 \,, \tag{15}$$

in which the functions g^1 and g^2 are independent. Then the available information related to H^1 is included in the available information related to H^2. Let S^1 be the maximum entropy related to H^1 with the constraint defined by Eq. (14) and S^2 be the maximum entropy related to H^2 with the constraint defined by Eq. (15). We then have

$$S^1 \geq S^2 \,. \tag{16}$$

By proceeding this manner, it is possible to create nested probabilistic model with increasing information (decreasing entropy).

3.1.2 Dependent information case

For this case, a correlation structure is introduced for the random field $\{H(\mathbf{x}), \mathbf{x} \in \Omega\}$ and, therefore, for the random vector $\mathbf{H}$. This correlation structure can be introduced through the Pearson correlation coefficient [6] defined by

$$\tilde{r}_H(\mathbf{x}, \mathbf{x}') = \frac{C_H(\mathbf{x}, \mathbf{x}')}{\sqrt{C_H(\mathbf{x}, \mathbf{x}) C_H(\mathbf{x}', \mathbf{x}')}}, \tag{17}$$

in which $C_H(\mathbf{x}, \mathbf{x}')$ is the covariance between $H(\mathbf{x})$ and $H(\mathbf{x}')$ defined by $C_H(\mathbf{x}, \mathbf{x}') = E\{(H(\mathbf{x}) - m_H(\mathbf{x}))(H(\mathbf{x}') - m_H(\mathbf{x}'))\}$ in which $m_H(\mathbf{x}) = E\{H(\mathbf{x})\}$. We then have $\tilde{r}_H(\mathbf{x}, \mathbf{x}) = 1$ for all $\mathbf{x}$ in Ω. Since it is assumed that the random field $\{H(\mathbf{x}), \mathbf{x} \in \Omega\}$ is homogeneous, the correlation coefficient is rewritten as

$$r_H(\mathbf{x} - \mathbf{x}') = \frac{C_H(\mathbf{0}, \mathbf{x} - \mathbf{x}')}{\sigma_H^2}, \tag{18}$$

in which $\sigma_H^2 = C_H(\mathbf{0}, \mathbf{0})$. In most of the correlation model that can be found in the literature, the correlation coefficient is isotropic and, therefore, only depends on the distance between $\mathbf{x}$ and $\mathbf{x}'$. For instance, the exponential correlation model is given by

$$r_H(\mathbf{x} - \mathbf{x}') = \exp\left(-\frac{\| \mathbf{x} - \mathbf{x}' \|}{l^2}\right), \tag{19}$$

in which l is a positive real variable. Now, let $[T_H]$ be the matrix defining the correlation coefficients for the N points where the stochastic process $\{H(\mathbf{x}), \mathbf{x} \in \Omega\}$ is discretized. We then have

$$[T_H]_{ij} = r_H(\mathbf{x}^i - \mathbf{x}^j). \tag{20}$$

The matrix $[T_H]$ completely defines the correlation structure of the random vector $\mathbf{H}$. In this paper, we will consider only cases where this matrix is positive-definite, although it can be positive semi-definite. The possible zero eigenvalues can be eliminated by introducing the regularization $[T_H^{\text{reg}}] = [T_H] + \alpha[I_N]$ in which $[I_N]$ is the identity matrix and where $0 < \alpha \ll 1$. The diagonal elements of matrix $[T_H]$ are equal to one and the other entries are lower than one. Therefore, using Hadamard inequality, it can be shown that

$$0 < \det([T_H]) \leq 1, \tag{21}$$

the equality arising for the uncorrelated case. In this paper, the homogeneous correlation length following the direction $\mathbf{e}_k$ is defined by

$$L_c^k = \int_0^{+\infty} |r_H(\eta \, \mathbf{e}_k)| \mathrm{d}\eta. \tag{22}$$

For instance, using the correlation model in Eq. (19) yields $L_c^1 = L_c^2 = L_c^3 = \sqrt{\pi} \, l/2$. Other definitions of the correlation length can be found in the literature [8].

The objective of this section is to take into account a correlation structure in the construction of the probability model of the random vector $\mathbf{H}$, which means that $\mathbf{H}$ has to verify $N(N-1)/2$ additional constraints defined for $1 \leq i \leq (N-1)$, $i < j \leq N$ by

$$E\{(H_i - m_{H_i})(H_j - m_{H_j})\} = \sigma_H^2 [T_{\mathrm{H}}^g]_{ij}, \tag{23}$$

in which the matrix $[T_{\mathrm{H}}^g]$ is the target value for $[T_{\mathrm{H}}]$ and where $m_H = E\{H\}$. There are several ways to take into account these constraints. Let us analyze three different ways.

(1) The first one consists in directly imposing the constraints defined by Eq. (23) in the construction of the MaxEnt distribution. This way is numerically prohibitive in high-stochastic dimension because it yields $N(N-1)/2$ additional Lagrange multipliers to be identified. Furthermore the components of the random vector $\mathbf{H}$ would be dependent and then the integrals involved in Eqs. (7), (12) and (13) could not be calculated using a numerical integration method. It should be noted that a new algorithm (see [18,2]) has recently been developed in order to address this problem in a relatively high stochastic dimension ($N < 10,000$).

(2) The second one consists in constructing the random vector $\mathbf{H}$ as a transformation of the independent (thus uncorrelated) random vector $\mathbf{H}^{\mathrm{nc}}$, obtained in Section 3.1, in the following way. Let the autocorrelation matrix of random vector $\mathbf{H}^{\mathrm{nc}}$ be $E\{(\mathbf{H}^{\mathrm{nc}} - \mathbf{m}_{\mathbf{H}^{\mathrm{nc}}})(\mathbf{H}^{\mathrm{nc}} - \mathbf{m}_{\mathbf{H}^{\mathrm{nc}}})^T\} = \sigma_H^2[I_N]$. The transformation is defined by

$$\mathbf{H} = [V](\mathbf{H}^{\mathrm{nc}} - \mathbf{m}_{\mathbf{H}^{\mathrm{nc}}}) + \mathbf{m}_{\mathbf{H}^{\mathrm{nc}}}, \tag{24}$$

in which $\mathbf{m}_{\mathbf{H}^{\mathrm{nc}}} = E\{\mathbf{H}^{\mathrm{nc}}\}$ and the matrix $[V]$ is related to the Cholesky factorization of matrix $[T_H]$, i.e, $[T_H] = [V][V]^T$. Then it can be verified that $E\{\mathbf{H}\} = \mathbf{m}_{\mathbf{H}} = \mathbf{m}_{\mathbf{H}^{\mathrm{nc}}}$ and $E\{(\mathbf{H} - \mathbf{m}_{\mathbf{H}})(\mathbf{H} - \mathbf{m}_{\mathbf{H}})^T\} = \sigma_H^2[T_H]$ and, therefore, Eq. (23) is verified. Nevertheless, the random vector $\mathbf{H}$ constructed using Eq. (24) does not verify the constraints defined by Eq. (6) which is verified only by the random vector $\mathbf{H}^{\mathrm{nc}}$. Furthermore, the transformation also modify the support of the probability distribution. Therefore, if the correlation between the components is strong, the construction defined by Eq. (24) is not adapted.

(3) The third way, which is the one adopted in the present work, consists in introducing a Nataf transformation [11,9,17] of the random vector $\mathbf{H}$. This transformation consists in introducing the following change of variable for each component of random vector $\mathbf{H}$

$$H_i = F_{H_i^{\mathrm{nc}}}^{-1}(\Phi(U_i)), \tag{25}$$

in which $U_1, \ldots, U_N$ are the components of the Gaussian centered random vector $\mathbf{U}$ for which the covariance matrix is denoted by $[C_U]$. In Eq. (25), the function $u \mapsto \Phi(u)$ is the cumulative distribution function of the normalized Gaussian random variable and the function $v \mapsto F_{H_i^{\mathrm{nc}}}^{-1}(v)$ is the reciprocal function of the cumulative distribution of the random variable H_i^{nc} which is

the ith component of the random vector $\mathbf{H}^{\text{nc}}$ constructed following Section 3.1. By construction, the random vector $\mathbf{H}$ verifies the constraints defined by Eq. (6). It can be shown that the joint probability density function of the random vector $\mathbf{H}$ is such that

$$p_{\mathbf{H}}(\mathbf{h}) = \frac{1}{\sqrt{\det([C_U])}} \exp\left(-\frac{\mathbf{u}(\mathbf{h})^T([C_U]^{-1} - [I_N])\mathbf{u}(\mathbf{h})}{2}\right) p_{\mathbf{H}^{\text{nc}}}(\mathbf{h}), \quad (26)$$

in which $\mathbf{u}(\mathbf{h}) = (\Phi^{-1}(F_{H_1^{\text{nc}}}(h_1)), \ldots, \Phi^{-1}(F_{H_N^{\text{nc}}}(h_N))$ and where the function $\mathbf{h} \mapsto p_{\mathbf{H}^{\text{nc}}}(\mathbf{h})$ is the probability density function of random vector $\mathbf{H}^{\text{nc}}$ constructed following the Section 3.1, which can be rewritten as

$$p_{\mathbf{H}^{\text{nc}}}(\mathbf{h}) = \prod_{i=1}^{N} p_{H_i^{\text{nc}}}(h_i), \quad (27)$$

in which the pdf $h \mapsto p_{H_i^{\text{nc}}}(h)$ is defined by Eq. (12). The correlation matrix $[C_U]$ has to be calculated such that the constraints defined by Eq. (23) is verified, yielding an inverse problem which is difficult to solve [9]. The direct choice $[C_U] = [T_H]$ generally gives very good results. For the classical pdfs, a correction of $[C_U]$ in order to improve the verification of Eq. (12) can be constructed [9] if necessary. It can be noted that the Pearson correlation coefficients for the random vector $\mathbf{H}$ and $\mathbf{U}$ are different but the Spearman rank correlation coefficients [6] for the random vectors $\mathbf{H}$ and $\mathbf{U}$, which are defined as the Pearson correlation coefficients for the random vectors $(F_{H_1^{\text{nc}}}(H_1^{\text{nc}}), \ldots, F_{H_N^{\text{nc}}}(H_N^{\text{nc}}))$ and $(\Phi(U_1), \ldots, \Phi(U_N))$, respectively, are equal by construction. In the rest of this paper, the approximation $[C_U] = [T_H]$ is chosen. Then, it can be proven that the entropy $S(p_{\mathbf{H}})$ of the pdf $p_{\mathbf{H}}$ is such that

$$S(p_{\mathbf{H}}) = S(p_{\mathbf{H}^{\text{nc}}}) + \frac{1}{2} \log(\det([T_H])). \quad (28)$$

Thus, using Eq. (22) it can be verified that

$$S(p_{\mathbf{H}}) \leq S(p_{\mathbf{H}^{\text{nc}}}), \quad (29)$$

the equality arising for the uncorrelated case. This means that even if the correlation has not been introduced directly during the construction of the MaxEnt distribution, it induces a decrease of the entropy anyway, as it corresponds to an additional information. In general, the value of $\log(\det([T_H]))$ depends on the correlation coefficient model and on the correlation length. For the 1-D version of the exponential correlation model introduced in Eq. (19) for a domain $[0, 1]$ discretized into 100 regularly spaced points, the function $L_c \mapsto \log(\det([T_H(L_c)]))$ is plotted on Fig. 1. It can be seen that this function decreases very rapidly, which means that as the correlation increases, the entropy decreases. This corresponds well to the intuition that the information of the probabilistic model increases when the correlation length increases.

Finally, generators of independent realization of random vector $\mathbf{H}$ can easily be constructed using Eq. (25) and classical generators of Gaussian centered random vectors.
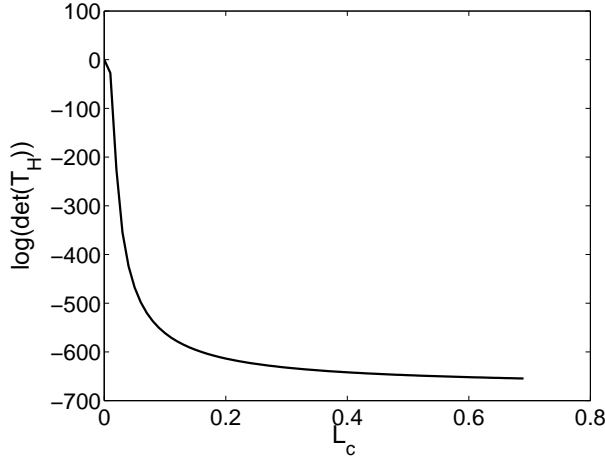
Fig. 1 Graph of the function $L_c \mapsto \log(\det([T_H(L_c)]))$.

3.2 Random response of the stochastic computational model

The stochastic computational is derived from the reduced nominal computational model introduced in Section 2.2, for which the deterministic vector $\mathbf{h}$ of the discretization of the uncertain fields is replaced by the random vector $\mathbf{H}$. Then, the n first random eigenvalues $0 < \Lambda_1(\mathbf{H}) \leq \ldots \leq \Lambda_n(\mathbf{H})$ associated with the random elastic modes $\{\psi_1(\mathbf{H}), \ldots, \psi_n(\mathbf{H})\}$ are solutions of the following random eigenvalue problem

$$[\mathrm{K}(\mathbf{H})]\,\psi(\mathbf{H}) = \Lambda(\mathbf{H})[\mathrm{M}(\mathbf{H})]\,\psi(\mathbf{H})\,. \tag{30}$$

Then for all ω in B, the random response $\mathbf{Y}(\omega)$ of the stochastic reduced-order computational model, is written as

$$\mathbf{Y}(\omega) = [\Psi(\mathbf{H})]\,\mathbf{Q}(\omega)\,, \tag{31}$$

in which the random vector $\mathbf{Q}(\omega)$ of the random generalized coordinates, is the solution of the following random reduced-order matrix equation,

$$(-\omega^2[\widetilde{M}(\mathbf{H})] + i\omega[\widetilde{D}(\mathbf{H})] + [\widetilde{K}(\mathbf{H})])\,\mathbf{Q}(\omega) = \mathbf{f}(\mathbf{H})\,. \tag{32}$$

This equation can be solved using the Monte Carlo simulation method [13]. The pdf of the random observation vector $\mathbf{Z} = OBS(\mathbf{Y}(\omega_1), \ldots, \mathbf{Y}(\omega_{n_{\mathrm{freq}}}))$ is denoted by $p_\mathbf{Z}$, and the observation entropy is defined by $S(p_\mathbf{Z}) = -\int_{\mathrm{R}^{n_{\mathrm{obs}}}} p_\mathbf{Z}(\mathbf{z})\,\log(p_\mathbf{Z}(\mathbf{z}))\mathrm{d}\mathbf{z}$. Let $\mathbf{Z}_1, \ldots, \mathbf{Z}_{n_s}$ be n_s independent realizations of the random observation vector $\mathbf{Z}$. Then, the observation entropy $S(p_\mathbf{Z})$ can be estimated using the plug-in estimator [3]

$$\widehat{S}(p_\mathbf{Z}) = -\frac{1}{n_s}\sum_{i=1}^{n_s}\log(\hat{p}_\mathbf{Z}(\mathbf{Z}_i))\,, \tag{33}$$

in which $\hat{p}_{\mathbf{Z}}$ is a multi-dimensional kernel density estimator for the random variable $\mathbf{Z}$. If $n_{\text{obs}} = 1$, then the entropy can also be estimated using a numerical integration of the integral $-\int_{A \subset \mathrm{R}} \log(\hat{p}_{\mathbf{Z}}(\mathbf{Z}))\hat{p}_{\mathbf{Z}}(\mathbf{Z})d\mathbf{Z}$, in which the compact support A can be delimited by the extremal values of the sampling $(\mathbf{Z}_1, \ldots, \mathbf{Z}_{n_s})$ for instance. For large values of n_{obs} the estimation of $\hat{p}_{\mathbf{Z}}$ using a multi-dimensional kernel density estimator becomes difficult. In this case, other estimators such as the nearest neighbour estimator [7] can be used. Another approach consists in introducing the variable $\mathbf{Z}^{\text{nc}} = [V]^{-1}\mathbf{Z}$, in which the matrix $[V]$ is related to the Cholesky factorization of the covariance matrix of random vector $\mathbf{Z}$, i.e, $E\{\mathbf{Z}\mathbf{Z}^T\} = [C_{\mathbf{Z}}] = [V][V]^T$. Then, the entropy of random vector $\mathbf{Z}$ is such that

$$S(p_{\mathbf{Z}}) = S(p_{\mathbf{Z}^{\text{nc}}}) + \frac{1}{2}\log(\det([C_{\mathbf{Z}}])). \tag{34}$$

It can be verified that the covariance matrix of $\mathbf{Z}^{\text{nc}}$ is the identity matrix and then the components of $\mathbf{Z}^{\text{nc}}$ are uncorrelated but dependent. By neglecting the dependence of the components of $\mathbf{Z}^{\text{nc}}$, the entropy $S(p_{\mathbf{Z}})$ of random vector $\mathbf{Z}$ can be approximated by a pseudo-entropy $\widetilde{S}(p_{\mathbf{Z}})$ defined by

$$\widetilde{S}(p_{\mathbf{Z}}) = \sum_{j=1}^{n_{\text{obs}}} S(p_{Z_j^{\text{nc}}}) + \frac{1}{2}\log(\det([C_{\mathbf{Z}}])), \tag{35}$$

which can be estimated using the plug-in estimator

$$\widehat{\widetilde{S}}(p_{\mathbf{Z}}) = -\frac{1}{n_s}\sum_{j=1}^{n_{\text{obs}}}\sum_{i=1}^{n_s}\log(\hat{p}_{Z_j^{\text{nc}}}(Z_{j,i}^{\text{nc}})) + \frac{1}{2}\log(\det(\frac{1}{n_s}\sum_{i=1}^{n_s}\mathbf{Z}_i\mathbf{Z}_i^T)) \tag{36}$$

in which $\hat{p}_{Z_j^{\text{nc}}}$ is a one-dimensional kernel density estimator for the random variable Z_j^{nc}. It should be noted that for Gaussian random vectors, the non-correlation implies the independence and, therefore, the entropy and the pseudo-entropy are equals, i.e., $S(p_{\mathbf{Z}}) = \widetilde{S}(p_{\mathbf{Z}})$.

4 Application

A clamped-clamped Euler-Bernoulli beam is considered for the application of entropy propagation. The beam has 1 meter length, diameter of 1×10^{-2} m, and material with Elastic Modulus of 210 GPa and density of 7850 kg/m³.

First, the nominal model and its deterministic response are presented, then the stochastic model is constructed from the nominal model and entropy propagation is analyzed.

4.1 Nominal model

The nominal computational is constructed as described in Section 2. The beam is discretized into 500 finite elements and Hermitian shape functions have been used. The frequency band of analysis is $B = [0, 314]$ kHz. Then the reduced-order model is constructed using 75 normal modes so that a good convergence of the response in frequency band B is reached. A proportional damping model with damping rate 0.01 has been used to construct the generalized damping matrix.

The first natural frequency of the structure is about 45 Hz. A vertical point force equal to one in the frequency band B is applied at $x = 0.70$ m. The frequency response in velocity $\{\omega \mapsto i\omega \times \mathbf{y}(\omega), \omega \in B\}$, with $i^2 = -1$, is calculated using Eqs.(4) and (5). The observation vector is the modulus of the transversal frequency response in velocity observed at $x = 0.40$ m and calculated for $n_{\text{freq}} = 20,000$ frequencies regularly spaced in the frequency band B. Figure 2a shows the values of this observation vector, and Fig. 2b shows a zoom in the low frequency band $[0, 3]$ kHz.

4.2 Stochastic model

The stochastic model is derived from the nominal model introduced in the previous section and for which the diameter is replaced by a random field yielding randomness in both the kinetic energy and elastic energy. Several random field models are successively introduced corresponding to successive addition of information. Four classes, which will be depicted in the next Section, are considered for the input probabilistic model: Uniform independent, Beta independent, Uniform correlated and Beta correlated.

4.2.1 Construction of the diameter random fields

The random fields are discretized at the middle of each element of the mesh, thus $N = 500$. The first diameter random field model corresponds to the case developed in Section 3.1.1 for which the components of random vector $\mathbf{H}^{\text{nc}}$ are independent. For this first model the available information is only related to the support $\mathcal{K}$ which is constrained to be $[\text{b}_{\text{low}}, \text{b}_{\text{up}}]$, in which $\text{b}_{\text{low}} = 0.75 \times 10^{-2}$ m is the lower bound and $\text{b}_{\text{up}} = 1.25 \times 10^{-2}$ m is the upper bound. Then applying MaxEnt principle yields a uniform distribution for the independent components of random vector $\mathbf{H}^{\text{nc}}$ denoted $\mathbf{H}^{\text{nc,unif}}$ for this first model, i.e., for i in $\{1, \ldots, N\}$

$$p_{H_i^{\text{nc,unif}}}(h_i) = \frac{1}{|\mathcal{K}|} \mathbb{1}_{\mathcal{K}}(h_i), \tag{37}$$

in which $|\mathcal{K}| = 5 \times 10^{-3}$ m is the size of the support $\mathcal{K}$. The entropy of the marginal distribution $p_{H_i^{\text{nc,unif}}}(h_i)$, called *marginal entropy* in this paper, is
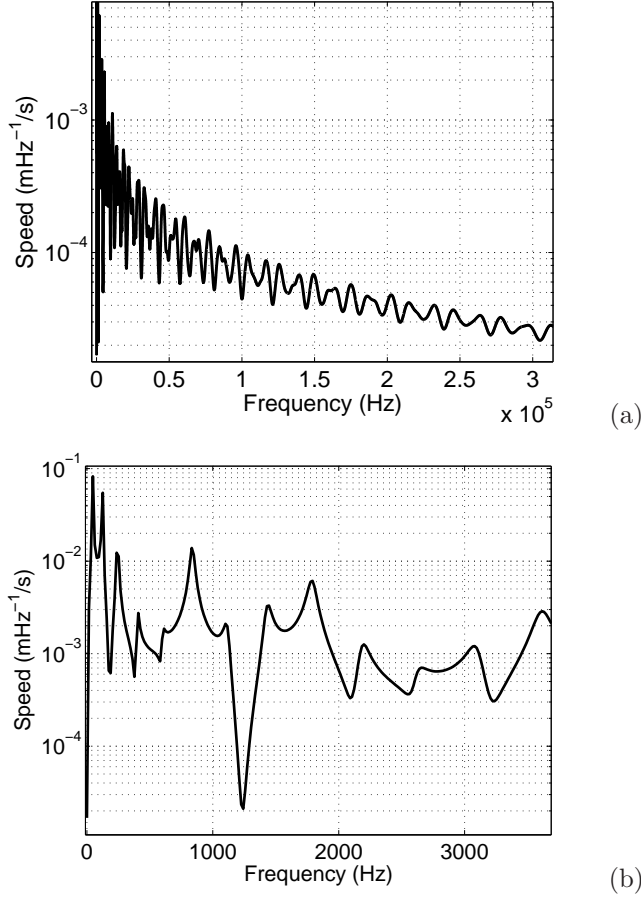
Fig. 2 Velocity spectrum of the deterministic response at $x = 0.40$. (a) $B = [0, 314]$ kHz and (b) $B = [0, 3]$ kHz.

then

$$S(p_{H_i^{\text{nc,unif}}}(h_i)) = \log(|\mathcal{K}|) \,, \tag{38}$$

which shows that the entropy (and then the uncertainty) increases as the length of the support increases. For the application, we then have $S(p_{H_i^{\text{nc,unif}}}(h_i)) \simeq -5.298$. Since the components of random vector $\mathbf{H}^{\text{nc,unif}}$ are independent, the total entropy of the distribution $p_{\mathbf{H}^{\text{nc,unif}}}$ of random vector $\mathbf{H}^{\text{nc,unif}}$ is $S(p_{\mathbf{H}^{\text{nc,unif}}}) = N \times S(p_{H_i^{\text{nc,unif}}}(h_i)) \simeq -2.65 \times 10^3$.

The second diameter random field model also corresponds to independent components. For this second model the available information is related to (1) the support $\mathcal{K}$ which is constrained to be $[\text{b}_{\text{low}}, \text{b}_{\text{up}}]$, (2) the behaviour of the pdf in the neighbourhood of the lower bound through the constraint

$E\{\log(H_i^{nc}-b_{low})\} = c_{low} < +\infty$ and (3) the behaviour of the pdf in the neighbourhood of the upper bound through the constraint $E\{\log(b_{up} - H_i^{nc})\} = c_{up} < +\infty$. Then applying MaxEnt principle yield a Beta distribution for the independent components of $\mathbf{H}^{nc}$ denoted $\mathbf{H}^{nc,beta}$ for this second model, i.e., for i in $\{1, \ldots, N\}$

$$p_{H_i^{nc,beta}}(h_i) = \frac{|\mathcal{K}|^{1-\alpha-\beta}}{\mathrm{B}(\alpha,\beta)} \, \mathbb{1}_{\mathcal{K}}(h_i)\, (H_i^{nc} - b_{low})^{\alpha-1}\, (b_{up} - H_i^{nc})^{\beta-1}, \quad (39)$$

in which $\alpha \geq 1$ and $\beta \geq 1$ depend on c_{low} and c_{up} and where $\mathrm{B}(\alpha,\beta)$ is the classical Beta function. The case $\alpha = 1$ and $\beta = 1$ is a special case which correspond to the uniform distribution and then corresponds to the first diameter random fields model. Instead of setting c_{low} and c_{up}, α and β are directly set to given values . The marginal entropy for $p_{H_i^{nc,beta}}(h_i)$ is then

$$\begin{aligned} S(p_{H_i^{nc,beta}}(h_i)) = {} & \log(|\mathcal{K}|) + \log(\mathrm{B}(\alpha,\beta)) - (\alpha-1)\,\Psi(\alpha) \\ & -(\beta-1)\,\Psi(\beta) + (\alpha+\beta-2)\,\Psi(\alpha+\beta), \end{aligned} \quad (40)$$

in which Ψ is the Digamma function defined by $\Psi(x) = \mathrm{d}(\log(\Gamma(x)))/\mathrm{dx}$ where $\Gamma(x)$ is the classical Gamma function. Then since $\alpha \geq 1$ and $\beta \geq 1$, we have as expected $S(p_{H_i^{nc,beta}}(h_i)) \leq S(p_{H_i^{nc,unif}}(h_i))$. For the application and for $\alpha = 2$ and $\beta = 2$, we then have $S(p_{H_i^{nc,beta}}(h_i)) \simeq -5.423$. The total entropy of the distribution $p_{\mathbf{H}^{nc,beta}}$ of random vector $\mathbf{H}^{nc,beta}$ is then $S(p_{\mathbf{H}^{nc,beta}}) = N \times S(p_{H_i^{nc,beta}}(h_i)) \simeq -2.71 \times 10^3$. 5000 independent realizations of random vectors $\mathbf{H}^{nc,unif}$ and $\mathbf{H}^{nc,beta}$ have been generated. It can be seen a good convergence of the plug-in estimators to the theoretical values.

The third diameter random field model corresponds to the case developed in Section 3.1.2 for which the components of random vector $\mathbf{H}$ are dependent. The available information for the components is the same as for the first diameter random field model. The correlation coefficient model is the Gaussian exponential one introduced in Eq. (19) with $l = 2\,L_c/\sqrt{\pi}$ in which L_c is the correlation length. Then the joint pdf of random vector $\mathbf{H}$ denoted $\mathbf{H}^{unif}$ for this third model is given by Eqs. (26) and (27) with $p_{H_i^{nc}}(h_i)$ defined by Eq. (37). Then the entropy of the marginal distribution are $p_{H_i^{nc}}(h_i) = p_{H_i^{nc,unif}}(h_i)$. The total entropy of the distribution $p_{\mathbf{H}^{unif}}$ of random vector $\mathbf{H}^{unif}$ is then $S(p_{\mathbf{H}^{unif}}) = N \times S(p_{H_i^{nc,unif}}(h_i)) + 0.5 \times \log(\det([T_H])) \leq S(p_{\mathbf{H}^{nc,unif}})$.

The fourth diameter random field model is constructed as the third diameter random field model but using marginal available information of the second diameter random field model. For this fourth model, the joint pdf of random vector $\mathbf{H}$ denoted $\mathbf{H}^{beta}$. We then have

$$S(p_{\mathbf{H}^{nc,unif}}) \geq S(p_{\mathbf{H}^{nc,beta}}) \geq S(p_{\mathbf{H}^{beta}}). \quad (41)$$

The same way, if the correlation length increases, the entropy decreases:

$$S(p_{\mathbf{H}^{nc,unif}}) \geq S(p_{\mathbf{H}^{unif,L_1}}) \geq S(p_{\mathbf{H}^{unif,L_2}}), \quad (42)$$

$$S(p_{\mathbf{H}^{\mathrm{nc,beta}}}) \geq S(p_{\mathbf{H}^{\mathrm{beta,L_1}}}) \geq S(p_{\mathbf{H}^{\mathrm{beta,L_2}}}), \tag{43}$$

where $L_1 < L_2$. The objective of the next section is to analyze whether this ordering is propagated to the stochastic dynamical responses of the beam. We expect the entropy of the response to increase if the entropy of the input random field increases.

4.2.2 Analysis of the random frequency responses

Let $\mathbf{Z}^{\mathrm{nc,unif}}$, $\mathbf{Z}^{\mathrm{unif}}$, $\mathbf{Z}^{\mathrm{nc,beta}}$ and $\mathbf{Z}^{\mathrm{beta}}$ be the random observation vectors corresponding to the four random vectors $\mathbf{H}^{\mathrm{nc,unif}}$, $\mathbf{H}^{\mathrm{unif}}$, $\mathbf{H}^{\mathrm{nc,beta}}$ and $\mathbf{H}^{\mathrm{beta}}$, respectively.

Concerning random vector $\mathbf{Z}^{\mathrm{nc,unif}}$, the random response is plotted on Fig. 3, with the 95% confidence envelope. Fig. 3b shows a zoom in the frequency band $[0, 3000]$Hz. It should be noted that the peaks of the mean random response are translated to the left, comparing with the response of the nominal model. For example, instead of a peak in about 830 Hz, the mean peak is about 760 Hz.

Figure 5 compares the marginal entropies for random vectors $\mathbf{Z}^{\mathrm{unif}}$ and $\mathbf{Z}^{\mathrm{beta}}$, for different correlation lengths. It can be seen as expected that $S(p_{Z_i^{\mathrm{nc,unif}}}) \geq S(p_{Z_i^{\mathrm{nc,beta}}})$ for almost all frequency ω_i. It should be noted that since the randomness introduced in the model translates the frequency response to lower or higher frequencies, the comparison is not strictly carried out frequency by frequency but peak by peak. For the uniform case, Fig. 4 shows the convergence of the L1-norm of the entropy response in the frequency band $[0, 314]$ kHz with respect the spatial discretization. It can be seen on this figure that, as expected, the convergence is faster for large correlation lengths. For the smallest correlation length ($L = 0.005$ m), a good convergence is reached for 500 beam elements (corresponding to 0.002 m for each beam element). Figure 6 details this response for different frequency bands. Since the upcoming conclusion is similar for $\mathbf{Z}^{\mathrm{unif}}$ and $\mathbf{Z}^{\mathrm{beta}}$, only $\mathbf{Z}^{\mathrm{unif}}$ is analyzed. Fig. 6a shows that, for low frequencies, the entropy of the response increases, as the correlation length increases, which is surprising with regard to the relation $S(p_{\mathbf{H}^{\mathrm{nc,unif}}}) \geq S(p_{\mathbf{H}^{\mathrm{unif}}})$. This result can be explained using stochastic homogenization theory (see [14], [17]): the size of the Representative Volume Element (RVE) increases with respect to the spatial correlation length. Therefore, for large wavelengths, the variability of the response increases with respect to the spatial correlation length and then the entropy increases. For higher frequencies, Fig. 6b, the spatial wavelengths of the mode shapes are smaller, therefore, no homogenization takes place any more and the expected result $S(p_{Z_i^{\mathrm{nc,unif}}}) \geq S(p_{Z_i^{\mathrm{unif}}})$ is obtained for each frequency ω_i. These results mean that in the low frequency band, the missing of the correlation structure information related to the input random fields is not conservative and can lead to an underestimation of the uncertainty related to the output response of the structure.
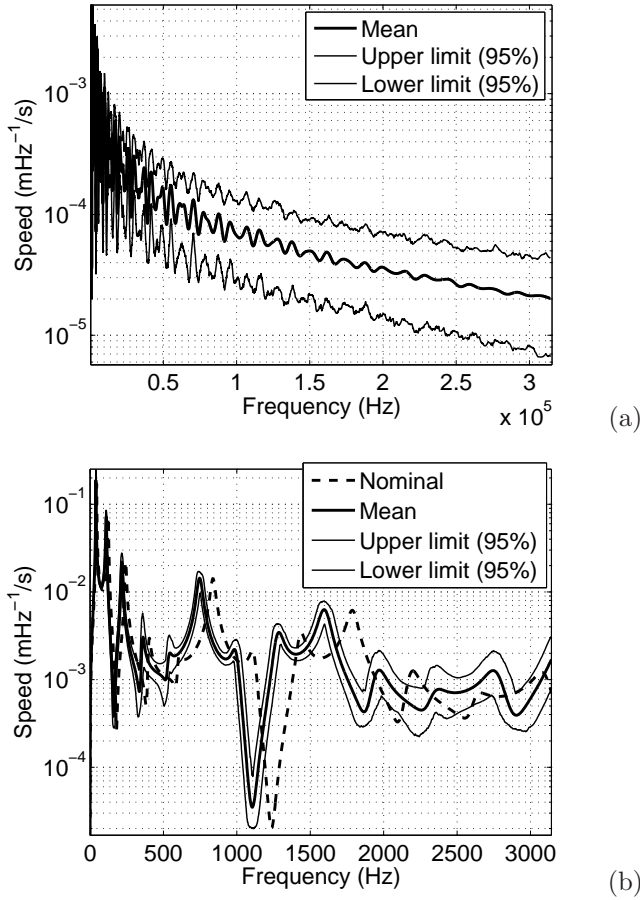
Fig. 3 Modulus of the velocity stochastic response $\mathbf{Z}^{\mathrm{nc,unif}}$ (a) and zoom in the low frequency band $[0, 3000]$Hz (b).

5 Conclusions

A methodology for the entropy propagation analysis in a dynamical structure has been presented. This methodology is based on the MaxEnt construction of the probability distribution of the input parameters with more or less information and in the estimation of the resulting entropy for quantities of interest. Concerning the application: (1) For the case of uncorrelated input random fields, the sensitivity of the output entropy with respect to the input entropy is low in the low frequency range but this sensitivity increases with respect to the frequency due to the decrease of the involved spatial wavelengths for the random displacement. (2) For the case of correlated input random fields, the output entropy increases as the correlation length increases (and then input
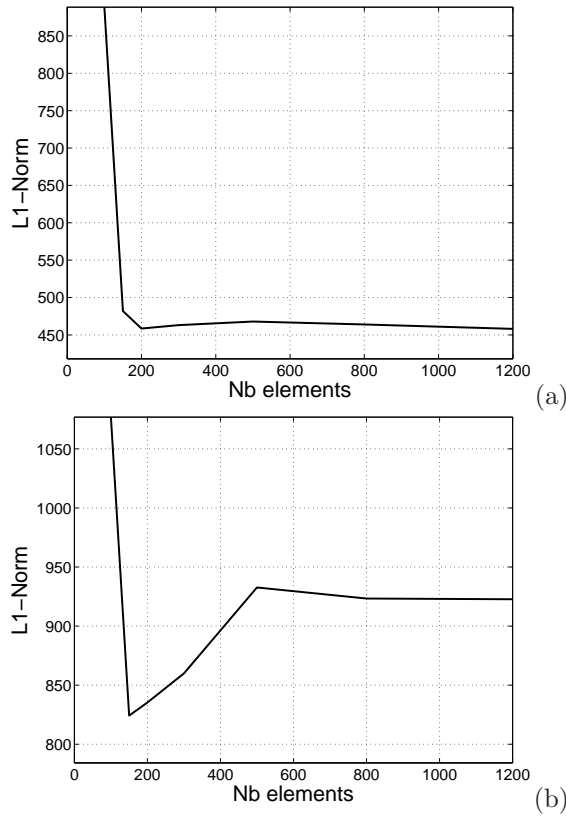
Fig. 4 For the uniform case, convergence analysis of the L1-norm of the entropy response in the frequency band $[0, 314]$ kHz with respect to the number of beam elements: (a) $L = 0.3$ m and (b) $L = 0.005$ m.

entropy decreases) in the low frequency range and decreases as the correlation length increases for higher frequencies. These results which can be explained by the stochastic homogenisation which takes place in the low frequency range show that the correlation structure of the input random fields has to be taken into account in order to avoid an underestimation of the output entropy. This result, which is not reachable using a classical variance-based sensitivity analysis is of primary importance for an engineering point of view and shows that a missing of information in the construction of the input probability model can underestimate the output uncertainty and then, in the case of a reliability analysis of a dynamical structure, the probability of failure can be underestimated.
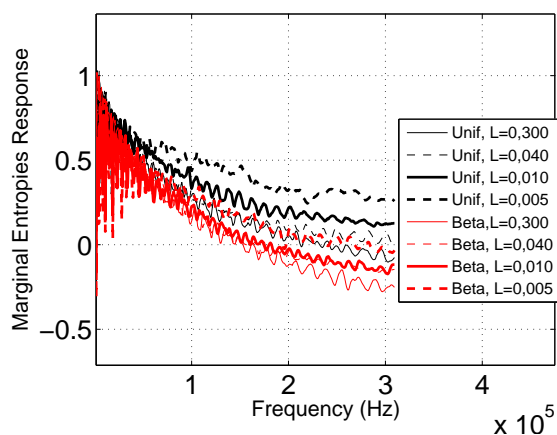
Fig. 5 Marginal entropies Marginal entropies for $\mathbf{Z}^{\mathrm{unif}}$ (black) and $\mathbf{Z}^{\mathrm{beta}}$ (red) for different correlation lengths.

References

1. M. Arnst, D. Clouteau, and M. Bonnet. Inversion of probabilistic structural models using measured transfer functions, Computer Methods in Applied Mechanics and Engineering, 197(6-8), 589-608 (2008).
2. A. Batou, C. Soize, Calculation of Lagrange Multipliers in the Construction of Maximum Entropy Distributions in High Stochastic Dimension, SIAM/ASA Journal on Uncertainty Quantification, 1(1), 431-451 (2013).
3. J. Beirlant, E. J. Dudewicz, L. Gyorfi, and E. C. van der Meulen, Nonparametric entropy estimation: An overview, International Journal of Mathematical and Statistical Sciences, 6, 17-39 (1997).
4. E. T. Jaynes, Information theory and statistical mechanics, Physical Review, 106(4), 620-630 and 108(2), 171-190 (1957);
5. J. N. Kapur, H. K. Kevasan, Entropy Optimization Principles with Applications. Academic Press, San Diego (1992).
6. G. Kendall and A. Stuart, The Advanced Theory of Statistics. Vol.2: Inference and Relationship. Griffin (1973).
7. L. F. Kozachenko and N. N. Leonenko, Sample estimate of entropy of a random vector, Problems of Information Transmission, 23, 95-101 (1987).
8. P. Krée and C. Soize, Mathematics of random phenomena. Reidel, Dordrecht (1986).
9. P. L. Liu, A. Der Kiureghian, 1986 Multivariate distribution models with prescribed marginals and covariances, Probabilistic Engineering Mechanics, 1(2), 105-112 (1986).
10. H. Liu, W. Chen, A. Sudjianto, Relative Entropy Based Method for Probabilistic Sensitivity Analysis in Engineering Design. Journal of Mechanical Design, 28(2), 326-336 (2005).
11. A. Nataf, Détermination des distributions de probabilités dont les marges sont données, Comptes Rendus de lAcadémie des Sciences, 225, 42-43 (1962).
12. J.M. Nichols, M. Seaver, and S.T. Trickey. A method for detecting damage-induced nonlinearities in structures using information theory, Journal of Sound and Vibration, 297(1-2), 1-16 (2006).
13. R Y. Rubinstein and D. P. Kroese , Simulation and the Monte Carlo Method. Simulation and the Monte Carlo Method, Wiley-Interscience, 2nd edition, (2007).
14. K. Sab, B. Nedjar, Periodization of random media and representative volume element size for linear composites. Comptes Rendus Mécanique, 333, 187-95 (2005).
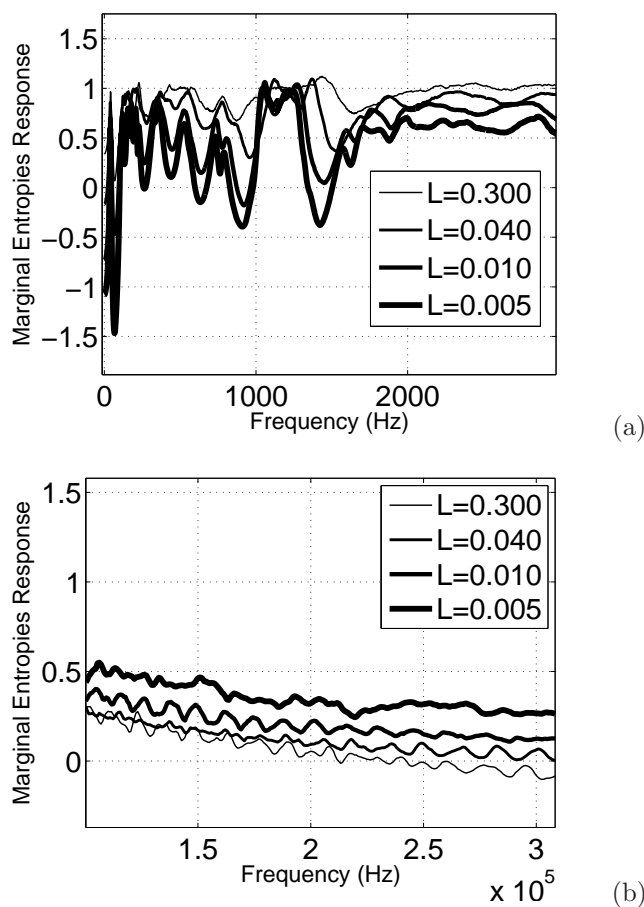
Fig. 6 Marginal entropies of the response for different correlation lengths of input Uniform probabilistic model. (a) low frequencies $[0, 3000]$ Hz and (b) high frequencies $[100, 300]$ kHz.

15. C. E. Shannon, A mathematical theory of communication, Bell System Technology Journal , 27, 379-423 and 623-659 (1948).
16. I.M. Sobol, Sensitivity estimates for nonlinear mathematical models. Mathematical Modelling and Computational Experiments, 1, 407-414 (1993).
17. C. Soize, Tensor-valued random fields for meso-scale stochastic model of anisotropic elastic microstructure and probabilistic analysis of representative volume element size. Probabilistic Engineering Mechanics 23(2-3), 307-323 (2008).
18. C. Soize, Construction of probability distributions in high dimension using the maximum entropy principle. Applications to stochastic processes, random fields and random matrices, International Journal for Numerical Methods in Engineering, 76(10), 1583-1611 (2008).